Available online at www.sciencedirect.com

Thin Solid Films 485 (2005) 82 – 89

www.elsevier.com/locate/tsf

Effects of oxygen pressure on lattice parameter, orientation, surface morphology and deposition rate of $(Ba_{0.02}Sr_{0.98})TiO_3$ thin films grown on MgO substrate by pulsed laser deposition

Can Wang[1], B.L. Cheng*, S.Y. Wang, H.B. Lu, Y.L. Zhou, Z.H. Chen, G.Z. Yang

Institute of Physics, Chinese Academy of Sciences, Beijing 100080, PR China

Received 15 August 2004; received in revised form 25 January 2005; accepted 24 March 2005

Abstract

$(Ba_{0.02}Sr_{0.98})TiO_3$ thin films were grown on MgO substrate by pulsed laser deposition (PLD) techniques at various oxygen pressures from 40 to 10^{-3} Pa. Effects of oxygen pressure on lattice parameter, orientation, surface morphology and deposition rate of the thin films were investigated. X-ray diffraction patterns indicate that, with decreasing oxygen pressure, crystal orientation of the thin films develops from (110) preferred orientation to random orientation, and finally to perfectly (00l) texture. Meantime, lattice parameter of the thin films increases with decreasing oxygen pressure. Especially, perfectly (00l)-oriented $(Ba_{0.02}Sr_{0.98})TiO_3$ thin film was obtained under oxygen pressure of 10^{-3} Pa at substrate temperature of 850 °C, in spite of the large lattice mismatch of about 8% between $(Ba_{0.02}Sr_{0.98})TiO_3$ and MgO. Atomic force microscopy images show that all the thin films have granular structure and the thin film grown at 10^{-3} Pa has much more homogeneous grain size distribution compared to all the other thin films. Moreover, the films grown at oxygen pressures of 1 and 10^{-1} Pa have more smooth surfaces, and the deposition rate of thin film increases with decreasing oxygen pressure.

PACS: 77.55; 68.55

Keywords: Oxygen pressure; Pulsed laser deposition; BST thin film; Structural characterization

1. Introduction

Thin films of $Ba_xSr_{1-x}TiO_3$ (BST) have recently been considered to be important materials for tunable microwave devices such as microwave tunable phase shifters, tunable filters, and high-Q resonators for radar and communication applications [1–3]. Tunable ferroelectric devices are generally used above the Curie temperature in paraelectric regime to reduce voltage hysteresis inherent to ferroelectric phase, and to lower dielectric loss because the ferroelectric phase introduces substantial intrinsic dielectric loss. BST thin films are considered to be the best candidate for this application because of their large electric field tunability, relatively low dielectric loss and variable Curie temperature. Transition temperature of BST from paraelectric to ferroelectric phase can be changed from 400 to 30 K by varying ratio of Ba/Sr, and it is favorable to obtain BST in paraelectric phase with good properties for use in specific temperature [4,5]. For example, to integrate high temperature superconductor thin films for high frequency system, high Sr composition BST should be selected for the microwave devices used at low temperature [1].

For the tunable microwave devices, it is very important to grow a thin film with high tunability and low dielectric loss. MgO is one of the best substrates for microwave applications because of its excellent dielectric properties such as a lower dielectric loss of about 3×10^{-7} and dielectric constant of about 9.7. These physical parameters of MgO compare well with those of Al_2O_3 ($\varepsilon \approx 10$, tan $\delta \approx 6 \times 10^{-5}$) or $LaAlO_3$ ($\varepsilon \approx 25$, tan $\delta \approx 6 \times 10^{-5}$) for microwave device applications. Unfortunately, there is a

---

* Corresponding author. Fax: +86 10 82649531.
E-mail address: blcheng@aphy.iphy.ac.cn (B.L. Cheng).

[1] Present address: Department of Earth Sciences, University of Cambridge, Downing Street, Cambridge, CB2 3EQ, UK.

0040-6090/$ - see front matter © 2005 Published by Elsevier B.V.
doi:10.1016/j.tsf.2005.03.055

large lattice misfit between BST (0.3905 nm for $SrTiO_3$) and MgO (0.4216 nm) substrate, especially in BST with rich Sr composition because the lattice constant of BST decreases with increasing Sr content, and also there is a difference in the thermal expansion coefficient (14×10^{-6}/K for MgO and 11×10^{-6}/K for $SrTiO_3$). Therefore, fabrication of high quality BST films on MgO substrate became a challenge. Pulsed laser deposition (PLD) technique has been regarded as one of the best methods for numerous advantages, including film stoichiometry close to the target, reproducibility, uniformity and simplicity, so it has been widely used in preparing ferroelectric thin films. Chen et al. [6] have reported that epitaxial $Ba_{0.6}Sr_{0.4}TiO_3$ thin films on MgO can only be achieved at temperature higher than 820 °C and under oxygen pressure in a narrow range between 200 and 300 mTorr. Kalyanaraman et al. [7] have investigated the growth of $SrTiO_3$ thin films on MgO substrates, and their results show that high quality thin films can only be grown at proper optimization temperature and oxygen pressure. Delage et al. [8] also investigated the microstructure and dielectric properties of BST thin films grown on MgO by PLD with and without buffer layer. Though many studies have reported BST thin film grown by PLD technique, systematic investigation on Sr-rich BST thin films on MgO substrate is still necessary to understand growth mechanism for fabricating high quality thin films.

As we know, oxygen vacancies, which affect the microstructure and properties of BST thin films, are introduced inevitably in the PLD-deposited oxide thin films for the lower deposition oxygen pressure. The lower the oxygen pressure, the higher the content of oxygen vacancies [9]. Moreover, existence of oxygen gas in the ambient has a strong influence on expansion of the laser-produced plasma plume and modifies the kinetic energy of the ablated species, resulting in difference on characteristics of thin film, such as surface morphology, growth rate, orientation, stoichiometric composition, etc. [10–14]. In this paper, elaboration and characteristics of $Ba_{0.02}Sr_{0.98}TiO_3$ films on MgO by PLD under a larger range of oxygen pressures are reported. It is found that lattice parameters, orientation, surface morphology and deposition rate of the thin films are sensitive to the ambient oxygen pressure.

2. Experimental details

Thin films of $(Ba_{0.02}Sr_{0.98})TiO_3$ were prepared by PLD technique employing a XeCl excimer laser with wavelength 308 nm, pulsed with 20 ns and frequency of 4 Hz. The laser with energy density of about 2 J/cm^2 was focused on ceramic target mounted on a motor-driving rotary stand rotating at a constant speed to ensure a uniform ablation rate. The ceramic target was prepared through conventional solid-state reaction process, using $BaCO_3$, $SrCO_3$ and TiO_2 with an analytic reagent grade of purity. Raw materials with stoichiometric composition of $(Ba_{0.02}Sr_{0.98})TiO_3$ were milled and then calcined at temperature of 950 °C. The calcined powders were pulverized and pressed into disk, then sintered at temperature of 1420 °C for 20 h. The thin films were grown on MgO (001) substrates with a distance of 4.5 cm between the substrate and target at 850 °C under oxygen pressures of 40, 10, 1, 10^{-1}, 10^{-2} and 10^{-3} Pa, respectively.

Crystallographic characteristics of the BST thin films were analyzed by X-ray diffraction (XRD) employing Cu Kα radiation (40 kV, 50 mA). Atomic force microscopy (AFM) was used to measure the surface morphology and roughness of the films, a randomly chosen area of 1×1 μm^2 on each film was surveyed. Thickness of the BST thin films was measured by a surface profile measuring system (DEKTAK III, USA) at a step grown by putting a mask on part of the substrate during deposition process.

3. Results and discussion

3.1. XRD patterns

Fig. 1 shows the XRD patterns of $(Ba_{0.02}Sr_{0.98})TiO_3$ thin films on MgO substrates deposited by PLD at oxygen pressures of 40, 10, 1, 10^{-1}, 10^{-2} and 10^{-3} Pa, respectively. As revealed from the XRD patterns, all peaks indexed in Fig. 1 correspond to perovskite phase, which indicates all $(Ba_{0.02}Sr_{0.98})TiO_3$ thin films well crystallized into single phase. Moreover, with decreasing growth oxygen pressure, intensities of (001) and (002) diffraction peaks are

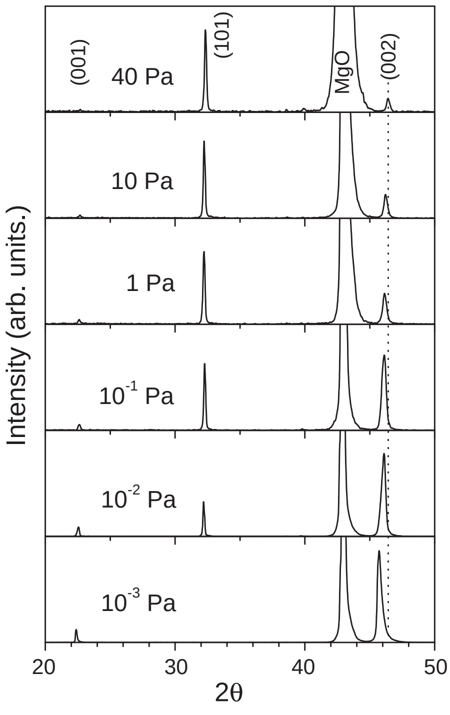

Fig. 1. XRD patterns of $(Ba_{0.02}Sr_{0.98})TiO_3$ thin films grown on MgO at various oxygen pressures by PLD.

increased, and (101) diffraction peak decreased. Significantly, XRD pattern of the thin film grown at 10^{-3} Pa exhibits only (00l) diffraction peaks, suggesting that a perfectly (00l)-oriented $(Ba_{0.02}Sr_{0.98})TiO_3$ thin film has been grown on MgO substrate.

3.2. Lattice parameter

As clearly shown in Fig. 1, the diffraction peaks shift to lower diffraction angle with decreasing oxygen pressure, which indicates an increase in lattice parameter. The variation of lattice constants of the $(Ba_{0.02}Sr_{0.98})TiO_3$ thin films grown under different oxygen pressures is given in Fig. 2. Here, the lattice constants are calculated from the distance of (002) planes, and actually, it is the lattice constant in the direction normal to the surface of the substrate, namely the out-of-plane lattice constant. At room temperature the $(Ba_{0.02}Sr_{0.98})TiO_3$ is in paraelectric phase with cubic structure. Though lattice distortion can be induced by interface stress from the larger lattice mismatch and thermal expansion mismatch between the thin film and MgO substrate, there is no obvious evidence of existence of other phase from the XRD patterns. This figure indicates that with decreasing oxygen pressure the lattice constant increases, i.e. the volume of unit cell increases.

The lattice constant of $(Ba_{0.02}Sr_{0.98})TiO_3$ thin films is larger than the lattice constant of 0.3906 nm for bulk material calculated from XRD patterns of ceramic target. The lattice constant of thin film in small thickness may enlarge by strain induced by the lattice mismatch and thermal expansion mismatch between thin film and substrate. But with increasing thickness, more and more dislocations should be generated to relieve the misfit strain, and as the thickness reaches a critical value of about 250 nm the strain will be completely relaxed and the lattice constant of thin film will approach to that of bulk material [15]. In our case, the film thickness is larger than the critical thickness of 250 nm so the misfit strain should be completely relaxed at the growth temperature through misfit dislocation. The lattice constant for the thin film grown at higher oxygen pressure of 40 Pa is 0.3911 nm, which is very closed to that of the bulk material. Therefore, the larger lattice constant in the $(Ba_{0.02}Sr_{0.98})TiO_3$ thin films grown at low oxygen pressure cannot be ascribed to the effect of misfit strain. Especially, the lattice constant is largely dependent on deposited oxygen pressure. Similar results were also observed in BST and $SrTiO_3$ thin films [8,16].

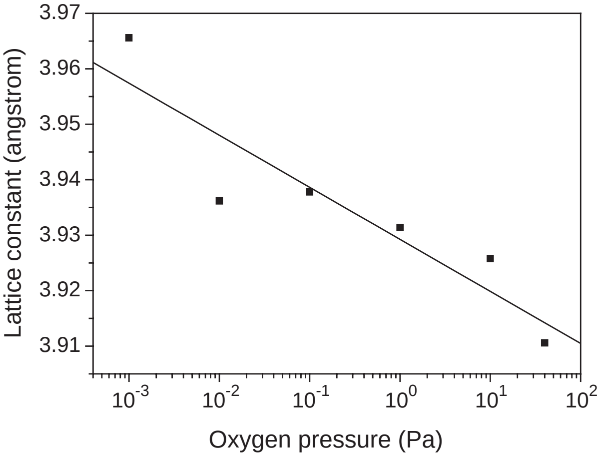

Fig. 2. Dependence of lattice parameter of $(Ba_{0.02}Sr_{0.98})TiO_3$ thin films on oxygen pressure.

The fact of increasing lattice constant with decreasing oxygen pressure suggests that the oxygen deficiency in the crystal lattice plays a dominant factor to enlarge the lattice constant. As the oxygen pressure during the growth of $(Ba_{0.02}Sr_{0.98})TiO_3$ thin films is very low, oxygen vacancies will be introduced in the $(Ba_{0.02}Sr_{0.98})TiO_3$ thin films inevitably. Indeed, the color of target surface became black after laser ablation at low oxygen pressure, which was an evidence of the oxygen loss. Zhao et al. [9] have measured the oxygen content in $BaTiO_3$ thin films by Rutherford backscattering spectrometry and show that the oxygen deficiency in thin film increases as the oxygen pressure decreases. Knauss et al. [17] have demonstrated that the lattice parameters of BST thin films decrease to the bulk lattice parameters after annealing in oxygen ambient which can cause an increase in oxygen stoichiometry for the thin film. The oxygen vacancies also play an important role in the electric conductivity of $BaTiO_3$, which is evident from its variation with oxygen pressure [9].

When the thin film grown at oxygen pressure below that corresponding to the stoichiometric composition, the oxide material of $(Ba_{0.02}Sr_{0.98})TiO_3$ will lose oxygen to stay in thermodynamic equilibrium with the ambient. The oxygen from the lattice will diffuse out as neutral atoms leaving behind its two electrons, resulting in an n-type conductivity in prepared BST thin films according to the following equation represented as

$$O_o = 1/2\ O_2 + V_o^{\circ\circ} + 2e'. \qquad (1)$$

This assumption is strongly supported by the work of Copel et al. [18]. The electrons resulting from the generation of oxygen vacancy can hop between different titanium ions in the perovskite structure, then the Ti^{3+} should appear in the thin film inevitably. Because the radius of Ti^{3+} is larger than that of Ti^{4+}, the increase of lattice constant should be related to the appearance of Ti^{3+}. The more oxygen vacancies, the more Ti^{3+} appears, so the lattice constant increases with the increase of oxygen vacancy concentration. In addition to that, as to the formation of oxygen vacancy, the nearest-neighbor atoms of oxygen vacancy will be displaced from ideal position because of the Coulombic electrostatic interactions of atoms [19,20]. For example, in $SrTiO_3$, the two Ti atoms and four Sr atoms will relax away from the vacant site, and the eight nearest-neighbor oxygen atoms will relax toward the vacant site [19]. Accordingly, the enlargement of lattice constants can also be related to the displacement of the nearest-neighbor atoms of oxygen vacancy, and the lattice constant will increase with the increase of the density of oxygen vacancies. Therefore, the enlargement of lattice constants of $(Ba_{0.02}Sr_{0.98})TiO_3$ thin film with decreasing oxygen pressure can be ascribed to the appearance of Ti^{3+} and the displacement of atoms in perovskite lattice resulting from the formation of oxygen vacancies.

3.3. Orientation

In order to analyze evolvement of preferred orientation of the thin film with variation of oxygen pressure, orientation factor is used to express the texture characterization of the thin films. Based on Lotgering's theory [21], the orientation factor can be defined as:

$$F = (P - P_0)/(1 - P_0) \tag{2}$$

$$P = \sum I_{(abc)} / \sum I_{(hkl)} \tag{3}$$

where F denotes the orientation factor with respect to a reference plane (abc) where abc denotes the Miller indices, P is for the textured thin film and means the ratio of the sum of intensities of the interested family of planes (abc) to the sum of all reflections, and P_0 stands for the equivalent ratio for ceramic powder of the target with random orientation. The value of the orientation factor for the preferred orientation is in the range of 0 and 1. An orientation factor of 0 indicates a randomly oriented film. As expected, large orientation factor F implies high texture, and $F = 1$ means complete preferred orientation.

The orientation factor of the thin films calculated from the XRD patterns is shown in Fig. 3 for (001) and (110) orientations as a function of oxygen pressure [for convenience, (110) is used here instead of (101) or (011)]. Here, P_0 is 0.28 for (00l) plane and 0.59 for (110) plane, which are calculated from the XRD intensities of the ceramic target. Diffraction peaks of 2θ from 20° to 50° in XRD patterns were used for the calculation of P and P_0. $F_{(00l)}$ increases with decreasing oxygen pressure. While the oxygen pressure is smaller than 1 Pa, the $F_{(00l)}$ is larger than 0, indicating that the thin film grown under lower oxygen pressure (from 10^{-1} to 10^{-3} Pa) is textured in (00l) preferred orientation. Furthermore, for the thin film grown under oxygen pressure of 10^{-3} Pa, $F_{(001)}$ is 1, which indicates that perfectly (00l)-oriented $(Ba_{0.02}Sr_{0.98})TiO_3$ thin film has been successfully grown on MgO substrate though the lattice misfit is larger than 8%. $F_{(110)}$ decreases with decreasing oxygen pressure, and while the oxygen pressure is larger than 1 Pa, the $F_{(110)}$ is larger than 0, which indicates that the thin film is textured in (110) preferred orientation. Moreover, at oxygen pressures of 1 and 10^{-1} Pa, both $F_{(100)}$ and $F_{(110)}$ are close to zero, suggesting that the thin films are almost grown in random orientation. Analysis of orientation factor gives us valuable information about the effect of oxygen pressure on texture orientation of thin film, i.e. the orientation of the $(Ba_{0.02}Sr_{0.98})TiO_3$ thin film developed from (110) preferred orientation to perfectly (001) orientation while the deposited oxygen pressure changed from 40 Pa to 10^{-3} Pa.

The dependence of film orientation on the oxygen pressure can be understood by status of the energy of ablated species and the lattice misfit. According to the bombardment mechanism [22], at a high oxygen pressure, the ablated species lose their initial energy due to multiple collisions between ablated species and oxygen species before reaching the substrate, and then the film is deposited by the low-energy scattered particles at oblique angles, resulting in a randomly oriented film. On the other hand, the particles ablated at lower oxygen pressure are expected to arrive at the substrate without significant loss of energy, and the film is deposited by high-energy particles normal to its surface, resulting in the film with a certain primary orientation. However, such picture cannot interpret growth of (110) preferred orientation thin film at higher oxygen pressure. In our case, the large lattice misfit between $(Ba_{0.02}Sr_{0.98})TiO_3$ and MgO results in large strain energy stored at interface, thus many misfit edge dislocations should be generated at interface to reduce total energy for the system, and aggregation of the dislocations must make it difficult to grow epitaxial BST thin films on MgO. Since a low-index plane possesses lower surface energy, it is more favorable to grow a film having a low-index plane parallel to the substrate surface. The $(Ba_{0.02}Sr_{0.98})TiO_3$ material has (110) plane as low-index plane, therefore at higher oxygen pressure the low energy ablated species is apt to grow film in (110) preferred orientation. As film is deposited at lower oxygen pressure, the film lattice parameter is enlarged by appearance of large amount of oxygen vacancies, and the lattice misfit and strain energy are reduced, thus it is easier for epitaxial growth of (001) thin film. In our case, both the higher-energy ablated species and the reduced lattice misfit are favored for the thin film grown in perfectly (001) orientation at the lower oxygen pressure of 10^{-3} Pa.

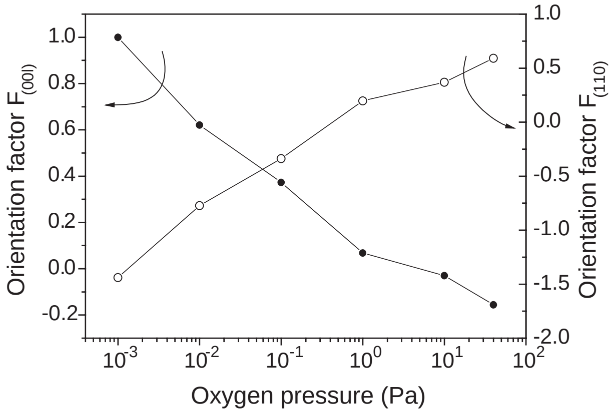

Fig. 3. Dependence of orientation factor of $(Ba_{0.02}Sr_{0.98})TiO_3$ thin films on oxygen pressure.

3.4. Surface morphology

Fig. 4 shows AFM images of the plane surface morphology. Fig. 5 shows the surface roughness of the $(Ba_{0.02}Sr_{0.98})TiO_3$ thin films. The surface roughness was determined for the thin films from the AFM images by the instrument's data analysis software. The root mean square (rms) surface roughness is defined by

$$\mathrm{rms} = \left[\frac{1}{N}\sum_{i-1}^{N}(Z_i - Z_a)^2\right]^{1/2} \tag{4}$$

where Z_i is the height of the ith point and Z_a is the arithmetic average height within the measurement area.

All the thin films show granular structure with grain size of about 100 nm. Fig. 4(a), for the thin film grown under 40 Pa, shows some mountains of the congeries of small club-shaped grains with very high surface roughness of 15 nm. With decreasing pressure, the mountains disappear and the surface becomes smooth as shown in Fig. 4(b), (c), (d), (e) and (f) for oxygen pressures of 10, 1, 10^{-1}, 10^{-2} and 10^{-3} Pa. The thin films grown at 1 and 10^{-1} Pa have much better smooth surface with surface roughness of about 0.5 nm. The thin films grown at 10^{-1} and 10^{-2} Pa show two different structures composed by a few spikes and flat pieces, and the grain size of these thin films seemingly has a larger distribution. According to the orientation factors shown in Fig. 3, it can be deduced that the spikes shown in Fig. 4(d) and (e) are oriented in (001) orientation and the flat pieces are in random orientation. With decreasing oxygen pressure, the spikes grow up, and the flat pieces dwindle in size then disappear finally. The thin film grown

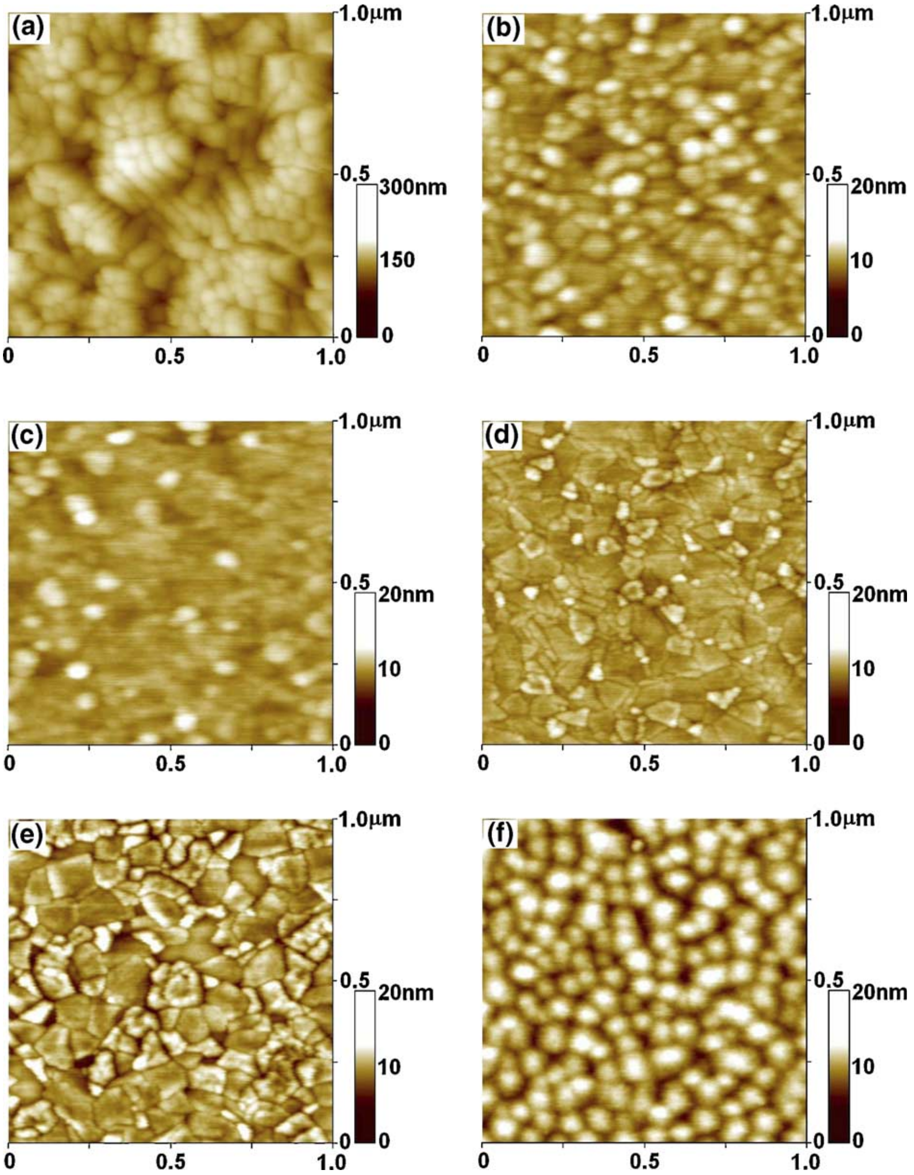

Fig. 4. AFM images of the surface of $(Ba_{0.02}Sr_{0.98})TiO_3$ thin films grown at various oxygen pressures. (a) 40 Pa, (b) 10 Pa, (c) 1 Pa, (d) 10^{-1} Pa, (e) 10^{-2} Pa and (f) 10^{-3} Pa.

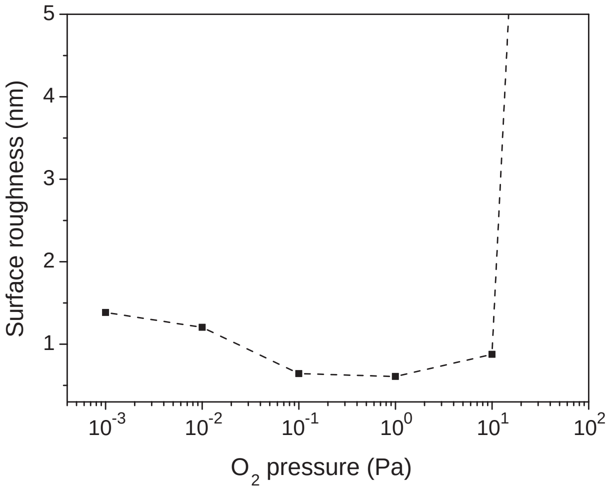

Fig. 5. Dependence of surface roughness of $(Ba_{0.02}Sr_{0.98})TiO_3$ thin films on oxygen pressure.

at 10^{-3} Pa shows a homogeneous granular structure with grain size of about 100 nm as shown in Fig. 4(f), and has a surface roughness of 1.4 nm. As shown in Fig. 5, the surface roughness decreases with decreasing oxygen pressure at oxygen pressure range from 40 to 1 Pa, and then the surface roughness increases slightly with further decreasing of oxygen pressure.

The surface roughness of thin films could be related to many parameters such as substrate temperature, ambient gas, deposition rate, etc. Lee at al. [23] reported that, with the increasing deposition flux, $LiNbO_3$ thin film surface became smooth with improved surface flatness. Study also shows the surface roughness of the $SrTiO_3$ thin films decreases with decreasing oxygen growth pressure and increasing substrate temperature [24]. Nakamura et al. show that the surface roughness of BST thin films on Pt grown at 133 Pa is much higher than that at 6.6 Pa [25]. In our case, the thin film grown at 40 Pa has a much higher surface roughness than other thin films. This shows an evidence of islands nucleate rather than growing in atomic layers. We assumed that there exists an energy barrier that must be conquered for the adatoms to move down to lower level at the edge of islands. If the energy of the ablated species is too low to conquer the energy barrier, which means lower adatom mobility, new islands will be formed on the islands and surface flatness will be deteriorated. At higher oxygen pressure of 40 Pa, the energy of ablated species is lower because of the scattering and multiple collisions between the ablated species and the oxygen species, and it could not conquer the energy barrier to jump down from the islands to smooth the surface. Furthermore, new grains are formed. Therefore, this thin film has the highest surface roughness and shows some mounts of the congeries of small grains. As the oxygen pressure decreases, the energy of the ablated species will increase. When the oxygen pressure is lower than 10 Pa, the energy of the species could be able to conquer the energy barrier to move down, so the surface roughness of these thin films grown under oxygen pressure lower than 10 Pa is improved significantly, and at the pressure range of 10 to 10^{-1} Pa, the surface roughness decreases with decreasing oxygen pressure. However, with further decrease of the pressure to 10^{-2} Pa, the surface roughness is increased slightly, which should be related to the preferred-orientation growth of the thin films for the surface roughness could be increased in the case of growth with a preferred orientation in a certain crystal plane.

3.5. Deposition rate

The deposition rate of the thin films grown at different oxygen pressures in the identical conditions, such as temperature, laser parameter, target distance, etc., is shown in Fig. 6. The deposition rate is calculated by the thickness of thin film and depositing time. It is clearly shown that the deposition rate of the thin film by PLD is increased with decreasing of oxygen pressure.

Many studies have investigated the film growth rate in PLD [12,25–27], and it is found that the growth rate is related to many parameters such as laser energy density, substrate temperature, target distance, gas pressure, etc. It should be noted that some contrary results have been reported about the dependence of growth rate on ambient gas pressure. This could be resulting from the different specific conditions in each experiment. Tyunina et al. [12] have revealed that there are different behaviors for the dependence of growth rate of PZT thin film on gas pressure: (1) at high laser fluence an increase in ambient gas pressure resulted in an increasing growth rate up to a maximum value, followed by a relative decrease; (2) while for a low laser fluence the growth rate decreased with increasing ambient gas pressure. The deposition process was treated as arrival of ablated species on the substrate surface, i.e. adsorption and desorption of some adatoms. The adatoms will diffuse over the substrate surface and combine into

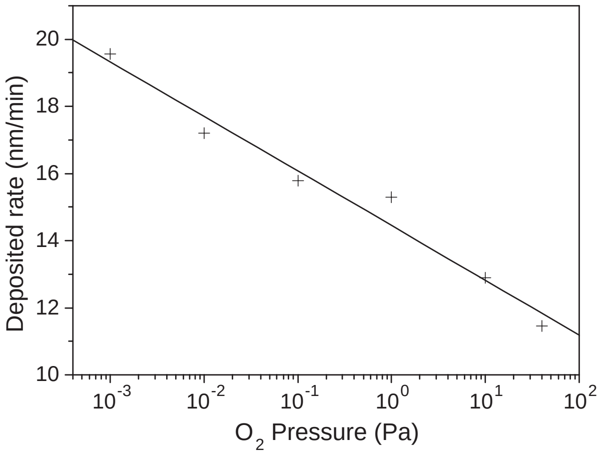

Fig. 6. Dependence of deposition rate of $(Ba_{0.02}Sr_{0.98})TiO_3$ thin films on oxygen pressure.

clusters or islands to form film. The film growth rate per laser pulse r_f can be expressed by [12]:

$$r_\mathrm{f} = \frac{1}{\rho} j_\mathrm{f} = \frac{1}{\rho} Aj\left[1 - \exp\left(-\frac{1}{a}\right)\right] \qquad (5)$$

$$a = \frac{k_\mathrm{B} T}{E_\mathrm{d}} \qquad (6)$$

where ρ is the density of thin film, j_f is the fraction of the flux of the ablated species, which remained on the surface as a result of adsorption–desorption processes and formed the film, A is a coefficient, j is the flux of the species arriving on the substrate after laser pulse: $j = nv$, where n is the density and v is the velocity of the species in the substrate vicinity, a is the parameter, characterizing the ability of adatoms to desorb, or the degree of surface activation, E_d is the activation energy of desorption, T is the temperature relating to the activated complex, and k_B is the Boltzmann constant. Here, we considered the film growth rate in the center of the plume and, correspondingly, v related to the forward directed motion of the species and their normal incidence on the substrate surface.

With decreasing gas pressure, the energy of the ablated species increases, corresponding to an increase in adatoms; probably it also led to an increase in the rate of desorption for the increase of adatom energy. Both the rate of arrival and the rate of desorption of the species in a gas pressure could finally determine the growth rate. In our case, we thought the rate of arrival of the ablated species is mainly the factor to influence deposition rate. At higher oxygen pressure, the ablated species are scattered by the multiple collisions between the ablated species and oxygen species, so propagation distance of the ablated species should be shortened, i.e. the number of particles that across the target distance and arrive to the substrate surface will be reduced. Nakata et al. [10] have demonstrated that expansion of the plume is influenced by ambient oxygen pressure and the velocity of ablated $\mathrm{BaTiO_3}$ particle at lower oxygen pressure is higher than that at higher oxygen pressure. On the contrary, at lower oxygen pressure, more high energy particles will arrive to the substrate. Therefore, the deposition rate of $\mathrm{(Ba_{0.02}Sr_{0.98})TiO_3}$ thin film increases with the decrease of oxygen pressure.

4. Conclusions

The influence of oxygen pressure on the growth of $\mathrm{(Ba_{0.02}Sr_{0.98})TiO_3}$ thin film on MgO substrate by PLD have been investigated in the oxygen pressure range from 40 to 10^{-3} Pa. It is revealed that the lattice parameter, film orientation, surface roughness, and deposition rate are dependent on the oxygen pressure. Especially, perfectly (00l)-oriented $\mathrm{(Ba_{0.02}Sr_{0.98})TiO_3}$ thin film, with homogeneous columnar microstructures and flat surface, has been fabricated under oxygen pressure of 10^{-3} Pa at substrate temperature of 850 °C, in spite of the large lattice mismatch of about 8% between $\mathrm{(Ba_{0.02}Sr_{0.98})TiO_3}$ and MgO. The major effects of oxygen pressure on the growth of thin films can be concluded as: First, lattice parameter of the thin films increases with decreasing oxygen pressure, which is mainly ascribed to the effect of increase of oxygen vacancy content rather than that of the interface strain resulting from the large lattice misfit between $\mathrm{(Ba_{0.02}Sr_{0.98})TiO_3}$ thin film and MgO. Second, with decreasing oxygen pressure, crystal orientation of the thin films develops from (110) preferred orientation to random orientation, and finally to perfectly (00l) texture. The increase of adatom energy and decrease of lattice misfit are thought to be favored for the growth of (001) texture film. Third, surface roughness of the thin film grown at 40 Pa is much higher than that of other films. It is explained by the fact that adatoms with lower energy cannot conquer the energy barrier to move down. At pressure range of 10 to 10^{-1} Pa, the surface roughness decreases with decreasing oxygen pressure. Further decreasing the pressure to 10^{-2} Pa, the surface roughness is increased slightly, which is related to the preferred-orientation growth of the thin films. Fourth, deposition rate of the thin film increases with decreasing oxygen pressure, because at low oxygen pressure the number of adatoms that remained on the surface as a result of adsorption–desorption processes is larger than that at higher oxygen pressure. This investigation suggests that oxygen pressure is an important factor to influence the growth of the thin films and can be manipulated to obtain thin film with designed characteristics.

Acknowledgements

The authors are very grateful for the financial support of the "Hundreds Talents Project" of the Chinese Academy of Sciences, the Chinese Postdoctoral Science Foundation, and the National Natural Science Foundation of China.

References

[1] F.W. Van Keuls, R.R. Romanofsky, D.Y. Bohman, M.D. Winters, F.A. Miranda, C.H. Mueller, R.E. Treece, T.V. Rivkin, D. Galt, Appl. Phys. Lett. 71 (1997) 3075.
[2] A.T. Findikoglu, Q.X. Jia, X.D. Wu, G.J. Chen, T. Venkatesan, D.W. Reagor, Appl. Phys. Lett. 68 (1996) 1651.
[3] A.T. Findikoglu, R. Camassa, G. Lythe, Q.X. Jia, Appl. Phys. Lett. 80 (2002) 3391.
[4] O.G. Vendik, S.P. Zubko, J. Appl. Phys. 88 (2000) 5343.
[5] S.V. Razumov, A.V. Tumarkin, M.M. Gaidukov, A.G. Gagarin, A.B. Kozyrev, O.G. Vendik, A.V. Ivanov, O.U. Buslov, V.N. Keys, L.C. Sengupta, X. Zhang, Appl. Phys. Lett. 81 (2002) 1675.
[6] C.L. Chen, J. Shen, S.Y. Chen, G.P. Luo, C.W. Chu, F.A. Miranda, F.W. Van Keuls, J.C. Jiang, E.I. Meletis, H.Y. Chang, Appl. Phys. Lett. 78 (2001) 652.

[7] R. Kalyanaraman, R.O. Vispute, S. Oktyabrsky, K. Dovidenko, K. Jagannadham, J. Narayan, J.D. Budai, N. Parikh, A. Suvkhanov, Appl. Phys. Lett. 71 (1997) 1709.

[8] T. Delage, C. Champeaux, A. Catherinot, J.F. Seaux, V. Madrangeas, D. Cros, Thin Solid Films 453–454 (2004) 279.

[9] T. Zhao, Z.H. chen, F. Chen, H.B. Lu, G.Z. Yang, H.S. Cheng, Appl. Phys. Lett. 77 (2000) 4338.

[10] Y. Nakata, G. Soumagne, T. Okada, M. Maeda, Appl. Surf. Sci. 127–129 (1998) 650.

[11] J. Gonzalo, R.G.S. Roman, J. Perriere, C.N. Afonso, R.P. Casro, Appl. Phys., A 66 (1998) 487.

[12] M. Tyunina, J. Levoska, S. Leppavuori, J. Appl. Phys. 83 (1998) 5489.

[13] J. Zhang, D. Cui, Y. Zhou, L. Li, Z. Chen, M. Szabadi, P. Hess, Thin Solid Films 287 (1996) 101.

[14] T. Zhao, F. Chen, H.B. Lu, G.Z. Yang, Z.H. Chen, J. Appl. Phys. 87 (2000) 7442.

[15] L.S.J. Peng, X.X. Xi, B.H. Moeckly, S.P. Alpay, Appl. Phys. Lett. 83 (2003) 4592.

[16] M. Hirarani, K. Imagawa, K. Takagi, Jpn. J. Appl. Phys. 34 (1995) 254.

[17] L.A. Knauss, J.M. Pond, J.S. Horwits, D.B. Chrisey, C.H. Mueller, R. Treece, Appl. Phys. Lett. 69 (1996) 25.

[18] M. Copel, P.R. Duncombe, D.A. Neumayer, T.M. Shaw, R.M. Tromp, Appl. Phys. Lett. 70 (1997) 3227.

[19] J.P. Buban, Hakim Iddir, S. Ogut, Phys. Rev., B 69 (2004) 180102.

[20] C.H. Park, D.J. Chadi, Phys. Rev., B 57 (1998) R13961.

[21] F.K. Lotgering, J. Inorg. Nucl. Chem. 9 (1959) 113.

[22] J.A. Thornton, J. Vac. Sci. Technol., A 4 (1986) 3059.

[23] G.H. Lee, B.C. Shin, B.H. Min, Mater. Sci. Eng., B 95 (2002) 137.

[24] R. Castro-Rodriguez, A.I. Oliva, M. Aguilar, P. Bartolo-Perez, E. Vasco, F. Leccabue, J.L. Penal, Appl. Surf. Sci. 125 (1998) 58.

[25] T. Nakamura, Y. Yamanaka, A. Morimoto, T. Shimizu, Jpn. J. Appl. Phys. 34 (1995) 5150.

[26] D.J. Lichtenwalner, O. Auciello, R. Dat, A.I. Kingon, J. Appl. Phys. 74 (1993) 7497.

[27] M. Tyunina, I.L. Sreenivas, C. Bjormander, J. Wittborn, K.V. Rao, Appl. Surf. Sci. 96–98 (1996) 831.